

# Thermochemical Behavior of Crystalline RE(Val)Cl<sub>3</sub>·6H<sub>2</sub>O (RE = Nd, Er, Val = Valine)<sup>†</sup>

Jing-Nan Zhang,<sup>‡,§</sup> Zhi-Cheng Tan,<sup>\*,‡,§</sup> Bei-Ping Liu,<sup>||</sup> Quan Shi,<sup>‡,§</sup> and Bo Tong<sup>‡,§</sup>

Thermochemistry Laboratory, Dalian Institute of Chemical Physics, Chinese Academy of Sciences, Dalian 116023, China, Graduate School of the Chinese Academy of Sciences, Beijing 100049, China, and Department of Chemistry, Hunan University of Arts and Science, Changde 415000, China

Heat capacities of two solid complexes of rare-earth elements with valine RE(Val)Cl<sub>3</sub>·6H<sub>2</sub>O (RE = Nd, Er, Val = Valine) have been measured with a high-precision automatic adiabatic calorimeter over the temperature range from (78 to 376) K. An anomaly of a large step in the heat capacity curve was detected in the temperature range of roughly (308 to 314) K and (297 to 300) K for the Nd and Er complex, respectively, which may be attributed to a glass transition corresponding to freezing of structural disorder. Thermal decomposition of the two complexes was studied by a thermogravimetric (TG) technique, and the possible mechanism for the decomposition was suggested.

## Introduction

Solid complexes of rare-earth elements with amino acids are important chemical substances, which are widely used in agriculture and the medicine industry. In 1975, Anghileri first reported that [La(Gly)<sub>3</sub>(H<sub>2</sub>O)]Cl<sub>3</sub>·3H<sub>2</sub>O has an antitumor effect.<sup>1</sup> Rare-earth complexes with amino acids have been extensively studied because of their physiological and biochemical effects. On the other hand, with the wide use of these complexes, rare-earth elements are inevitably spread into the food chain and then into the bodies of human beings. To obtain information about the long-term effects of rare-earth elements on people, the complexes of lanthanide ions with amino acids as ligands have been synthesized and extensively studied by a variety of methods.<sup>2–6</sup> However, until now, the study of thermochemical properties of many solid complexes of rare-earth complexes with amino acids has been unsystematized and even absent.

In the present work, the low-temperature heat capacities of two complexes, Nd(Val)Cl<sub>3</sub>·6H<sub>2</sub>O and Er(Val)Cl<sub>3</sub>·6H<sub>2</sub>O, were measured over the temperature range from (78 to 376) K. In the course of the experiment, a large step in heat capacities was detected for both complexes, and the possible cause for the anomaly in heat capacities is discussed. In addition, possible mechanisms of thermal decompositions of the two complexes are proposed on the basis of thermogravimetric (TG) analysis.

## Experimental Section

According to the literature,<sup>7</sup> rare-earth oxides (Nd<sub>2</sub>O<sub>3</sub>, Er<sub>2</sub>O<sub>3</sub>, > 99.9 %, purchased from Shanghai Chemical Reagent Co., Ltd., in China), hydrochloric acid, and valine were used to prepare the experimental samples. First, the rare-earth oxides were dissolved in hydrochloric acid to get the aqueous solutions of the rare-earth chlorides, and then the aqueous solutions were

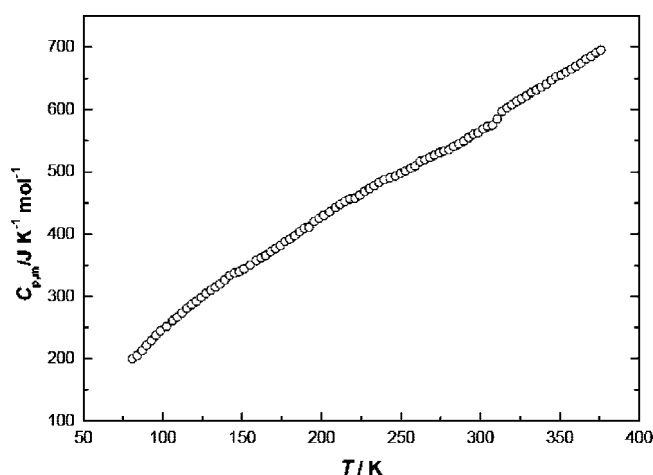


Figure 1. Experimental molar heat capacities of Nd(Val)Cl<sub>3</sub>·6H<sub>2</sub>O as a function of temperature.

mixed with valine at the mole ratio of 1:1 at about pH = 3, which was regulated by adding a suitable amount of NaOH. The mixed solution was concentrated by evaporation, cooled, and filtered. The filtrate was placed into a desiccator with P<sub>2</sub>O<sub>5</sub> until crystalline products isolated from the solutions. The crystals were filtered out and washed with anhydrous alcohol three times. After this procedure, the color changed to purple and pink crystals. Finally, these crystals were desiccated in a dryer until their mass became constant.

The mass fraction of the crystals was proved to be more than 99.90 % by EDTA titrimetric analysis, good enough to meet the requirements of the present calorimetric study.

A precision automatic adiabatic calorimeter was used to measure the heat capacities over the temperature range from (78 to 376) K. The calorimeter was established in the Thermochemistry Laboratory of the Dalian Institute of Chemical Physics, Chinese Academy of Sciences. The principle and structure of the adiabatic calorimeter have been described in detail elsewhere.<sup>8–10</sup> The heating duration and temperature increment for each experimental heat capacity point were usually

\* Corresponding author. E-mail address: tzc@dicp.ac.cn. Fax: +86-411-84691570. Tel. +86-411-84379199.

<sup>†</sup> Part of the special issue "Robin H. Stokes Festschrift".

<sup>‡</sup> Chinese Academy of Sciences.

<sup>§</sup> Graduate School of the Chinese Academy of Sciences.

<sup>||</sup> Hunan University of Arts and Science.

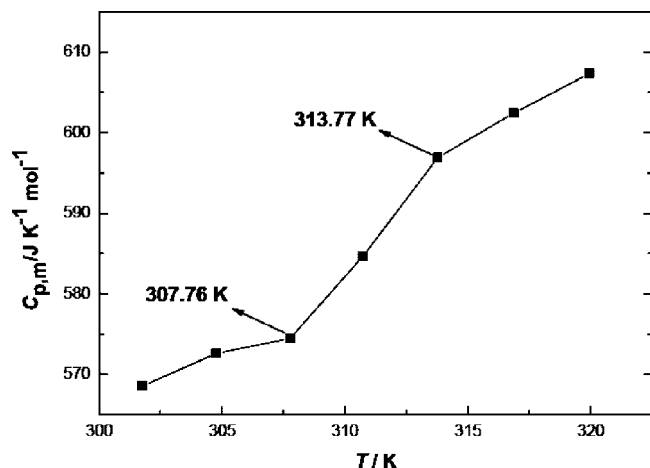


Figure 2. Experimental molar heat capacities of  $\text{Nd(Val)Cl}_3 \cdot 6\text{H}_2\text{O}$  in the temperature range of glass transition.

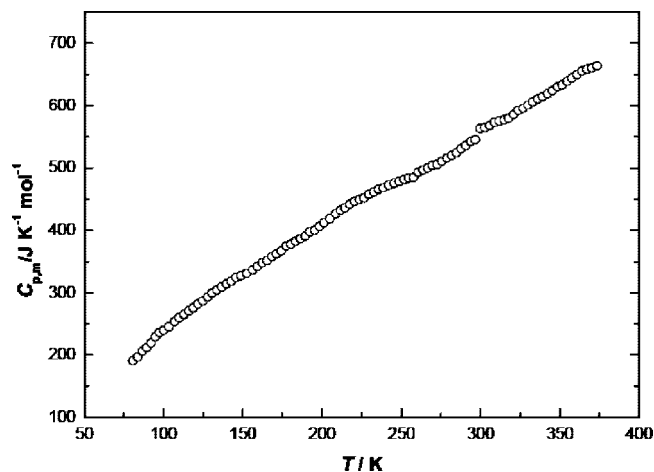


Figure 3. Experimental molar heat capacities of  $\text{Er(Val)Cl}_3 \cdot 6\text{H}_2\text{O}$  as a function of temperature.

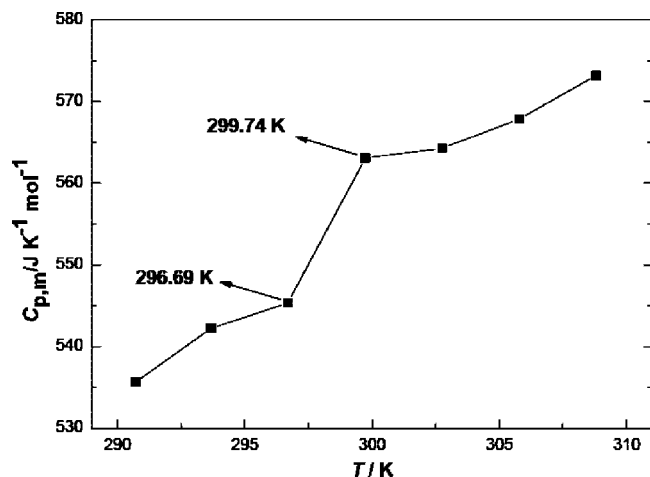


Figure 4. Experimental molar heat capacities of  $\text{Er(Val)Cl}_3 \cdot 6\text{H}_2\text{O}$  in the temperature range of glass transition.

controlled to be about 10 min and (1 to 3) K, respectively, during the whole experimental process.

Prior to the heat capacity measurements of the sample, the reliability of the calorimetric apparatus was verified by heat capacity measurements on the reference standard material,  $\alpha\text{-Al}_2\text{O}_3$ . The deviations of our experimental values from those of the smoothed curve lie within  $\pm 0.2\%$ , while the uncertainty is within  $\pm 0.3\%$ , as compared with the recommended values

Table 1. Experimental Molar Heat Capacities of  $\text{Nd(Val)Cl}_3 \cdot 6\text{H}_2\text{O}$  ( $M = 475.860 \text{ g} \cdot \text{mol}^{-1}$ )

$T$ K	$C_{p,m}$ $\text{J} \cdot \text{K}^{-1} \cdot \text{mol}^{-1}$	$T$ K	$C_{p,m}$ $\text{J} \cdot \text{K}^{-1} \cdot \text{mol}^{-1}$
80.91	199.57	230.23	472.85
84.04	205.11	233.28	477.43
87.00	213.18	236.37	482.90
89.92	221.62	239.47	486.96
92.86	229.03	243.07	490.31
95.77	237.43	246.69	493.18
98.62	244.94	249.82	497.58
102.43	251.53	252.92	501.05
106.32	261.26	256.02	505.60
109.26	266.90	259.10	508.83
112.22	273.55	262.17	516.34
115.22	280.70	265.21	519.03
118.21	286.79	268.24	522.90
121.18	291.99	271.25	526.87
124.19	298.08	274.25	530.69
127.19	304.28	277.24	533.32
130.19	309.75	280.29	535.12
133.18	314.89	283.41	540.41
136.17	319.83	286.51	544.30
139.17	326.15	289.59	549.06
142.16	333.55	292.65	554.88
145.21	337.59	295.69	560.26
148.25	339.59	298.73	562.56
151.26	344.31	301.75	568.52
155.12	350.03	304.76	572.57
158.95	357.73	307.76	574.44
161.93	361.70	310.74	584.68
164.93	365.68	313.77	596.89
167.96	371.76	316.87	602.42
171.02	376.55	319.95	607.32
174.05	381.57	323.03	612.92
177.06	388.22	326.09	617.19
180.12	391.79	329.15	621.64
183.19	397.33	332.20	627.00
186.23	403.83	335.24	631.33
189.24	409.59	338.36	635.75
192.29	410.93	341.54	640.27
195.36	420.38	344.69	646.80
198.40	425.32	347.83	652.39
201.42	429.74	350.98	655.42
205.13	435.49	354.12	660.12
208.84	442.21	357.23	664.56
211.84	447.77	360.32	668.97
214.90	452.39	363.39	674.32
218.00	456.29	366.53	680.81
221.10	457.37	369.68	685.21
224.18	462.41	372.84	690.75
227.23	468.26	375.99	695.15

reported by Archer<sup>11</sup> of NIST in the temperature range from (80 to 405) K.

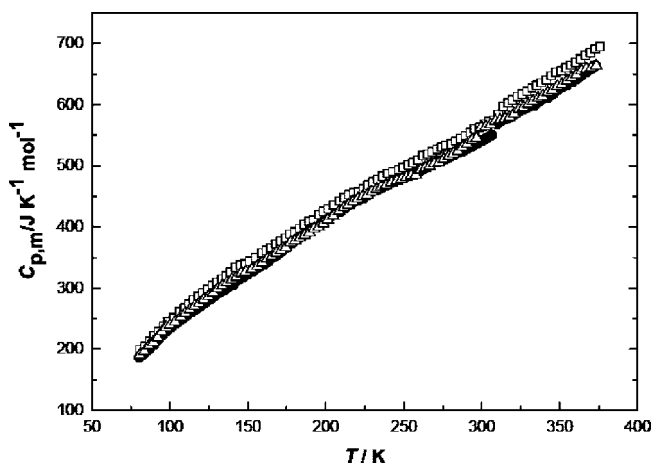
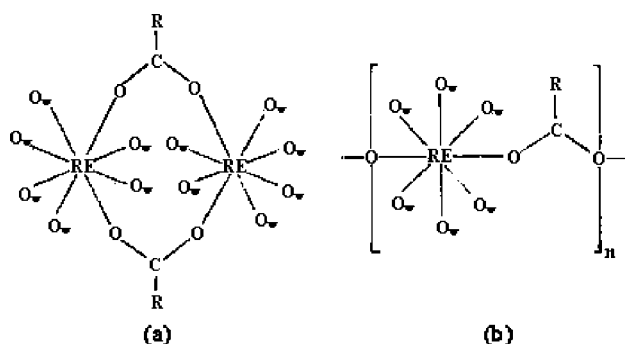


Figure 5. Experimental molar heat capacities of  $\text{RE(Val)Cl}_3 \cdot 6\text{H}_2\text{O}$  (RE = Nd, Sm, Er) as a function of temperature.  $\square$ ,  $\text{Nd(Val)Cl}_3 \cdot 6\text{H}_2\text{O}$ ;  $\bullet$ ,  $\text{Sm(Val)Cl}_3 \cdot 6\text{H}_2\text{O}$ ;  $\triangle$ ,  $\text{Er(Val)Cl}_3 \cdot 6\text{H}_2\text{O}$ .

**Table 2.** Experimental Molar Heat Capacities of  $\text{Er}(\text{Val})\text{Cl}_3 \cdot 6\text{H}_2\text{O}$  ( $M = 498.880 \text{ g} \cdot \text{mol}^{-1}$ )

$T$ K	$C_{p,m}$ $\text{J} \cdot \text{K}^{-1} \cdot \text{mol}^{-1}$	$T$ K	$C_{p,m}$ $\text{J} \cdot \text{K}^{-1} \cdot \text{mol}^{-1}$
80.76	190.58	229.55	457.85
83.72	196.75	232.53	461.56
86.63	205.81	235.55	465.61
89.45	211.95	238.56	468.08
92.18	219.37	242.06	472.49
94.84	229.26	245.59	475.67
97.45	235.92	248.65	478.49
100.00	239.46	251.71	481.49
103.44	245.37	254.75	483.78
107.07	253.58	257.76	484.67
109.98	259.59	260.75	493.31
112.92	265.18	263.73	496.66
115.87	270.66	266.69	499.66
118.86	275.48	269.64	503.90
121.83	281.48	272.64	505.48
124.81	286.40	275.70	510.60
127.77	292.58	278.74	515.59
130.73	299.62	281.77	520.08
133.72	304.13	284.77	524.07
136.71	309.03	287.76	530.81
139.70	314.07	290.73	535.68
142.70	318.25	293.68	542.19
145.68	324.13	296.69	545.35
148.71	327.12	299.74	563.08
152.53	330.83	302.75	564.23
156.33	336.32	305.77	567.84
159.33	341.93	308.79	573.16
162.36	347.97	311.81	575.10
165.37	351.45	314.82	576.94
168.35	357.89	317.82	579.64
171.31	362.08	320.81	585.35
174.31	366.82	323.80	592.04
177.34	374.64	326.85	595.81
180.34	377.61	329.95	600.40
183.36	382.51	333.06	606.04
186.34	386.75	336.16	610.45
189.35	390.46	339.24	614.16
192.38	397.34	342.33	619.27
195.39	399.81	345.40	624.04
198.37	405.98	348.48	629.86
201.33	411.98	351.55	633.21
204.98	418.16	354.63	639.03
208.64	426.27	357.71	644.15
211.63	431.74	360.80	649.44
214.61	435.80	363.95	655.09
217.55	441.62	367.16	658.44
220.55	446.21	370.37	660.38
223.59	449.21	373.57	663.73
226.60	452.03		

The mass of the  $\text{Nd}(\text{Val})\text{Cl}_3 \cdot 6\text{H}_2\text{O}$  and  $\text{Er}(\text{Val})\text{Cl}_3 \cdot 6\text{H}_2\text{O}$  used for heat capacity measurements was (3.77704 and 2.67576) g, which are equivalent to (0.00793729 and 0.00536353) mol, based on their corresponding molar mass of (475.860 and 498.880)  $\text{g} \cdot \text{mol}^{-1}$ , respectively.



**Figure 6.** Sketch map of the crystal structure of solid complexes of monovalino-hexaquo-rare-earth chlorides:<sup>7</sup> (a) dinuclear complexes; (b) one-dimensional chain complexes of infinite length.

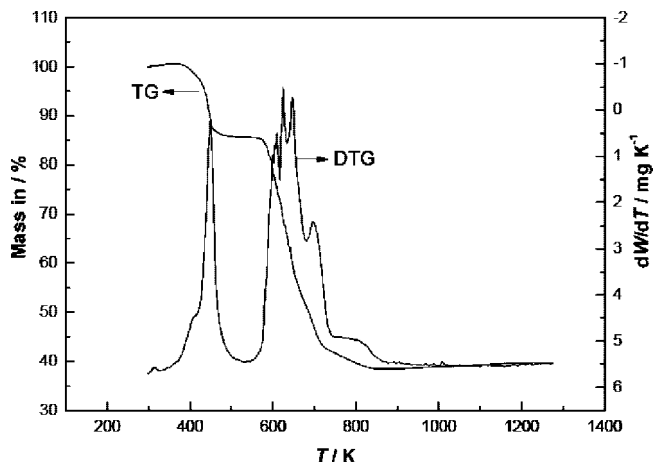


**Figure 7.** TG/DTG curve of  $\text{Nd}(\text{Val})\text{Cl}_3 \cdot 6\text{H}_2\text{O}$  under nitrogen atmosphere. Mass in is the leaving mass of the sample in percent.

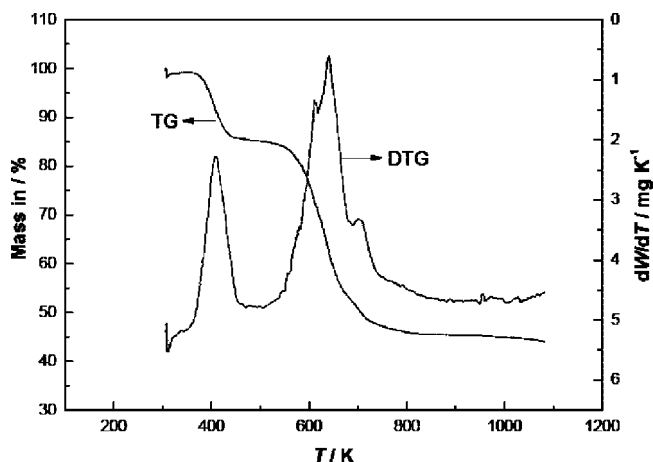


**Figure 8.** TG/DTG curve of  $\text{Er}(\text{Val})\text{Cl}_3 \cdot 6\text{H}_2\text{O}$  under nitrogen atmosphere.

A thermogravimetric analyzer (model DT-20B, Shimadzu, Japan) was used for TG measurements of the solid complexes under high-purity (99.999 %) nitrogen atmosphere with a flow rate of  $80 \text{ mL} \cdot \text{min}^{-1}$ . The masses of the samples used for TG analysis were (9.75 and 7.94) mg for  $\text{Nd}(\text{Val})\text{Cl}_3 \cdot 6\text{H}_2\text{O}$  and  $\text{Er}(\text{Val})\text{Cl}_3 \cdot 6\text{H}_2\text{O}$ , respectively. The heating rate was  $10 \text{ K} \cdot \text{min}^{-1}$ .

## Results and Discussion

**Heat Capacity.** The experimental molar heat capacities obtained by the adiabatic calorimeter over the temperature range from (78 to 376) K are shown in Figure 1 and Figure 3 and tabulated in Tables 1 and 2, respectively. The molar heat capacities of the samples are fitted to the following polynomials in reduced temperature ( $X$ ) by means of the least-squares fitting.

For the solid complex  $\text{Nd}(\text{Val})\text{Cl}_3 \cdot 6\text{H}_2\text{O}$ :

The temperature range from (80 to 305) K:

$$C_{p,m}/(\text{J} \cdot \text{K}^{-1} \cdot \text{mol}^{-1}) = 414.29322 + 174.72171X - 21.33248X^2 + 10.88861X^3 - 9.38797X^4 \quad (1)$$

where  $X$  is the reduced temperature  $X = [T - (T_{\max} + T_{\min})/2]/[(T_{\max} - T_{\min})/2]$ , where  $T$  is the experimental temperature. Thus, in the temperature range (80 to 305) K,  $X = [(T/\text{K}) - 192.5]/112.5$ ;  $T_{\max}$  is the upper limit (305 K); and  $T_{\min}$  is the lower limit (80 K) of the above temperature region. The

correlation coefficient of the fitting  $R^2 = 0.9996$ , and the fitness bias is 0.069 %.

The temperature range from (315 to 376) K:

$$C_{p,m}/(\text{J}\cdot\text{K}\cdot\text{mol}^{-1}) = 647.16612 + 46.46817X - 0.04272X^2 + 1.65301X^3 + 0.44314X^4 \quad (2)$$

where  $X$  is the reduced temperature,  $X = [(T/\text{K}) - 345.5]/30.5$ . The correlation coefficient of the fitted curve  $R^2 = 0.9995$ , and the fitness bias is 0.022 %.

For the solid complex  $\text{Er}(\text{Val})\text{Cl}_3\cdot 6\text{H}_2\text{O}$ :

The temperature range from (80 to 295) K:

$$C_{p,m}/(\text{J}\cdot\text{K}\cdot\text{mol}^{-1}) = 390.55819 + 165.657X - 15.59736X^2 - 6.2679X^3 - 11.16731X^4 \quad (3)$$

where  $X$  is the reduced temperature,  $X = [(T/\text{K}) - 187.5]/107.5$ . The correlation coefficient of the fitted curve  $R^2 = 0.9990$ , and the fitness bias is 0.084 %.

The temperature range from (303 to 376) K:

$$C_{p,m}/(\text{J}\cdot\text{K}\cdot\text{mol}^{-1}) = 615.0706 + 60.0485X + 2.82339X^2 - 9.63372X^3 - 1.8531X^4 \quad (4)$$

where  $X$  is the reduced temperature,  $X = [(T/\text{K}) - 339.5]/36.5$ . The correlation coefficient of the fitted curve  $R^2 = 0.9987$ , and the fitness bias is 0.040 %.

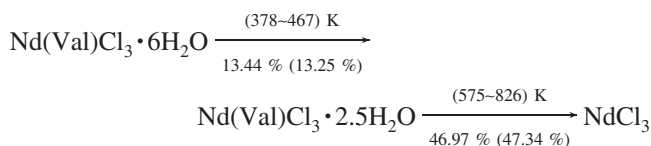
From Figure 1 and Figure 3, it can be seen that the heat capacities of the two complexes increase with temperature in a smooth and continuous manner in the temperature range from (80 to 305) K and from (315 to 376) K for  $\text{Nd}(\text{Val})\text{Cl}_3\cdot 6\text{H}_2\text{O}$  and from (80 to 295) K and from (303 to 374) K for  $\text{Er}(\text{Val})\text{Cl}_3\cdot 6\text{H}_2\text{O}$ . However, as we can see in Figures 2 and 4, a large step in heat capacity was detected around (313 and 299) K for  $\text{Nd}(\text{Val})\text{Cl}_3\cdot 6\text{H}_2\text{O}$  and  $\text{Er}(\text{Val})\text{Cl}_3\cdot 6\text{H}_2\text{O}$ , respectively; this may be attributed to a glass transition corresponding to freezing of structural disorder. Some studies<sup>12,13</sup> indicated that the glass transition is considered to arise from freezing of the orientational disorder. The presence of a glass transition indicates that there exists a configurational degree of freedom with plural distinguishable positions and/or orientations (of molecules or ions) which are separated with a large potential barrier and each of which has an appreciable temperature change in the occupation fraction in the transition region.<sup>13</sup> It should be noted that the anomaly in heat capacities of rare-earth chlorides with valine was not reported before the present calorimetric investigations. To understand the mechanism of the anomaly, the study for such compounds needs to be carried out further; meanwhile, when we carried out calorimetric investigation on  $\text{Sm}(\text{Val})\text{Cl}_3\cdot 6\text{H}_2\text{O}$ , there was a similar anomaly in the heat capacity curve where a large step was detected around 308 K.

**Comparison of Heat Capacity of  $\text{RE}(\text{Val})\text{Cl}_3\cdot 6\text{H}_2\text{O}$  ( $\text{RE} = \text{Nd}, \text{Sm}, \text{Er}$ ).** The experimental molar heat capacities of  $\text{RE}(\text{Val})\text{Cl}_3\cdot 6\text{H}_2\text{O}$  ( $\text{RE} = \text{Nd}, \text{Sm}, \text{Er}$ ) are shown in Figure 5. It is obvious that the experimental molar heat capacities of  $\text{Sm}(\text{Val})\text{Cl}_3\cdot 6\text{H}_2\text{O}$  and  $\text{Er}(\text{Val})\text{Cl}_3\cdot 6\text{H}_2\text{O}$  are very close. We considered that it may arise from the similarity of crystal structures between  $\text{Sm}$  and  $\text{Er}$  complexes. Researchers<sup>7</sup> concluded that the  $\text{Nd}$  complex was a one-dimensional chain complex of infinite length, whereas  $\text{Sm}$  and  $\text{Er}$  were dinuclear complexes. The sketch map of the crystal structure of these complexes is shown in Figure 6.

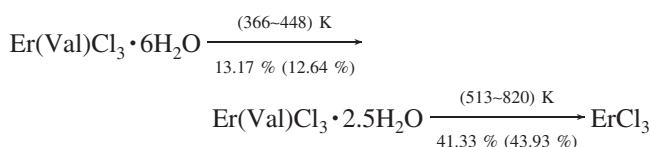
On the other hand, we noticed that the temperature at which the anomaly in heat capacities occurred has some certain orderliness: the temperature decreases with the increase of the atomic number of rare earth.

**TG Results.** The TG curve of  $\text{Nd}(\text{Val})\text{Cl}_3\cdot 6\text{H}_2\text{O}$  is shown in Figure 7. It can be seen clearly from the mass-loss curve that most of the activities occur in the temperature range of (575~826) K. The solid complex was stable below 373 K and started decomposition at 378 K. The total mass-loss (%) is 46.97 %. We consider that the residue should be  $\text{NdCl}_3$  because the mass-loss (%) calculated theoretically is 47.34 % if the final residual is  $\text{NdCl}_3$ .

Figure 8 shows that the structure of  $\text{Er}(\text{Val})\text{Cl}_3\cdot 6\text{H}_2\text{O}$  is stable below 363 K. It starts mass-loss at 366 K. The experimental result of final relative mass-loss was 41.33 %, which suggested that the residual product should be  $\text{ErCl}_3$  because the theoretical relative mass loss of the decomposition is 43.93 % when the final residual is  $\text{ErCl}_3$ . According to the mass-loss in each step, possible mechanisms of the thermal decompositions may be as follows



and



## Literature Cited

- (1) Anghileri, L. J. On the antitumor activity of gallium and lanthanides. *Arzneim.-Forsch.* **1975**, *25*, 793-795.
- (2) Zheng, Z. P. Ligand-controlled self-assembly of polynuclear lanthanide-oxo/hydroxo complexes: from synthetic serendipity to rational supramolecular design. *Chem. Commun.* **2001**, 2521-2529.
- (3) Xu, H.; Chen, L. Study on the complex site of L-tyrosine with rare-earth element  $\text{Eu}^{3+}$ . *Spectrochim. Acta, Part A* **2003**, *59*, 657-662.
- (4) Takada, J.; Nishimura, K.; Akaboshi, M. Element content in a number of plant leaves and accumulation of some elements in typical plant species. *J. Radioanal. Nucl. Chem.* **1997**, *217*, 65-70.
- (5) Glowiak, T.; Legendziewicz, J.; Huskowska, E.; Gawryszewska, P. Ligand chirality effect on the structure and its spectroscopic consequences in  $[\text{Ln}_2(\text{Ala})_4(\text{H}_2\text{O})_8](\text{ClO}_4)_6$ . *Polyhedron* **1996**, *15*, 2939-2947.
- (6) Csoregh, L.; Kierkegaard, P.; Legendziewicz, J.; Huskowska, E. Crystal structure of apraseodymium glutamate perchlorate hydrate,  $\text{Pr}_2(\text{L-Glu})_2(\text{ClO}_4)_4\cdot 11\text{H}_2\text{O}$ . *Acta Chem. Scand., Ser.* **1987**, *A41*, 453-460.
- (7) Ma, A. Z.; Li, L. M.; Xi, S. Q. Syntheses and infrared spectra of solid complexes of monovalino-hexaquo-rare earth chlorides. *Chin. J. Appl. Chem.* **1995**, *12*, 48-51.
- (8) Tan, Z. C.; Sun, L. X.; Meng, S. H.; Li, L.; Zhang, J. B. Heat capacities and thermodynamic functions of p-chlorobenzoic acid. *J. Chem. Thermodyn.* **2002**, *34*, 1417-1429.
- (9) Tan, Z. C.; Sun, G. Y.; Song, Y. J.; Wang, L.; Han, J. R.; Wang, M. An adiabatic calorimeter for heat capacity measurement of small samples—The heat capacity of nonlinear optical materials  $\text{KTiOPO}_4$  and  $\text{RbTiOAsO}_4$  crystals. *Thermochim. Acta* **2000**, 252-253, 247-253.
- (10) Tan, Z. C.; Sun, G. Y.; Sun, Y.; Yin, A. X.; Wang, W. B.; Ye, J. C.; Zhou, L. X. An adiabatic low-temperature calorimeter for heat capacity measurement of small samples. *J. Therm. Anal.* **1995**, *45*, 59-67.
- (11) Archer, D. G. Thermodynamic properties of synthetic sapphire ( $\alpha\text{-Al}_2\text{O}_3$ ), standard reference material 720 and the effect of temperature-scale differences on thermodynamic properties. *J. Phys. Chem. Ref. Data* **1993**, *22*, 1441-1453.
- (12) Tan, Z. C.; Nakazawa, Y.; Saito, K.; Sorai, M. Heat capacity and glass transition of crystalline pentachloronitrobenzene. *Bull. Chem. Soc. Jpn.* **2001**, *74*, 1221-1224.
- (13) Yukawa, Y.; Igarashi, S.; Masuda, Y.; Oguni, M. Phase transition and glass transition concerning configurational order/disorder of ions in crystalline  $(\text{TMA})_2[\text{Sr}\{\text{Ni}(\text{pro})_2\}_6](\text{ClO}_4)_4$  and  $(\text{TMA})[\text{Sm}\{\text{Ni}(\text{pro})_2\}_6](\text{ClO}_4)_4$ . *J. Mol. Struct.* **2002**, *605*, 277-290.

Received for review June 16, 2008. Accepted August 1, 2008. The authors are grateful to the National Natural Science Foundation of China for providing financial support (NSFC No.20373072 and 20753002) to this research project.